Novel Raman-Active Electronic Excitations near the Charge-Transfer Gap in Insulating Cuprates

Ran Liu,[1,*] D. Salamon,[1] M. V. Klein,[1] S. L. Cooper,[1] W. C. Lee,[1] S-W. Cheong,[2] and D. M. Ginsberg[1]

[1]*Science and Technology Center for Superconductivity, Department of Physics, and Materials Research Laboratory, University of Illinois at Urbana-Champaign, 104 S. Goodwin Avenue, Urbana, Illinois 61801*

[2]*AT&T Bell Laboratories, Murray Hill, New Jersey 07974*

(Received 27 May 1993)

We have observed electric-dipole-forbidden electronic excitations with A_{2g}, B_{1g}, and A_{1g} symmetries at energies near the charge-transfer gap in insulating cuprates, using large-shift Raman techniques. The strongest feature, with pseudovector A_{2g} symmetry, occurs in insulating cuprates just below the main optical absorption peak, varying from 0.15 to 0.2 eV below according to the Cu coordination number. $YBa_2Cu_3O_{6+x}$ spectra at different doping levels show that all the new features are suppressed in metallic phases. We propose two possible interpretations: internal d^9-d^9 and charge-transfer d^9-$d^{10}\underline{L}$ excitations.

PACS numbers: 74.25.Gz, 74.72.−h, 78.30.Hv

The search for microscopic mechanisms responsible for the unusual normal and superconducting states of the high-T_c cuprates would be aided by a comprehensive understanding of the parent insulating phase. While it is widely accepted that some version of the Hubbard model is an appropriate starting point for a description of the CuO_2 planes [1], questions remain as to its adequacy. For low-energy processes, there is intensive debate on the merits of the multiband extended versus the simplified one-band Hubbard models [2], but for excitation energies of the order of the charge-transfer (CT) energy one will need a multiband picture. Even multiband Hubbard models do not, however, take into account intra-atomic Cu d-d excitations. These excitations have not been identified experimentally to date, but were suggested by Weber [3] as the coupling mechanism for forming Cooper pairs in the high-T_c cuprates. The ground state of the CT insulators, as revealed by neutron diffraction experiments [4], is known to have long range antiferromagnetic order within the CuO_2 planes, but with a reduced Cu magnetic moment. Theoretically, it approximates the Néel phase, apart from local fluctuations into quantum-spin-liquid states such as the resonating-valence-bond state [5], or various flux phases [6].

Information from current experiments on the CT insulators is still very limited. High-energy spectroscopic [7] studies indicate that the lowest unoccupied states are formed from Cu $d_{x^2-y^2}$ orbitals and the highest unoccupied states from O p orbitals, but give both insufficient energy resolution and little information about electron-hole correlation effects. Optical absorption [8] probes such electron-hole pair excitations. In a typical insulating cuprate, the charge-transfer band is characterized by an abrupt rise in optical absorption forming a peak at about 1.7 eV, followed by weaker absorption extending beyond 4 eV. The above techniques do not, however, yield much information about pair excitations having symmetries other than E_u. Because electronic structure from outside the CuO_2 planes can mix into the same energy range as the Hubbard bands, it is difficult to reconcile experimental data with the Hubbard picture in the absence of such symmetry information. Recently, resonant Raman scattering (RRS) has been used to explore CT excitations in the insulating cuprates. Specifically, the behavior of both one-phonon [9], and two-phonon and two-magnon [10,11] features as the energy of the exciting laser photon is tuned through the CT band depends on the couplings of optical phonons and magnons to excitations forming the various portions of the band.

In this Letter, we explore interband excitations near the fundamental absorption edge in insulating cuprates using high-energy ordinary Raman scattering. This method, which to our knowledge has not previously been pursued (even for semiconductors), can reveal excitations inaccessible to other spectroscopies. Preliminary results from our work have previously been presented [11,12].

Our $RBa_2Cu_3O_{6+x}$ (R=Y,Pr) and R_2CuO_4 (R=Gd,Nd) single crystals were grown by using the CuO flux method [13]. As grown, the $RBa_2Cu_3O_{6+x}$ crystals had $x \approx 0.3$. After annealing at 650 °C for two days in flowing N_2, the oxygen content was reduced to $x < 0.1$. The untwinned $T_c = 66$ K ($x \approx 0.6$) and 90 K ($x \approx 1$) $YBa_2Cu_3O_{6+x}$ crystals were obtained by annealing the as-grown samples in flowing O_2 [13]. By exciting the materials with ultraviolet (UV) laser lines at 3.81 eV (3250 Å) from a He-Cd laser, at 3.71 eV (3345 Å), 3.53 eV (3511 Å), and 3.41 eV (3638 Å) from an Ar^+ laser, we took spectra out to very large Raman shifts (~2 eV) using a Spex Triplemate spectrometer with a liquid-nitrogen-cooled charge-couple device (CCD) detector. Measurements were made on very clean surfaces, because the UV laser can excite strong luminescence from any contamination on the sample surface. Several sets of samples of $YBa_2Cu_3O_{6+x}$ were used. We found that the surfaces of fresh samples are quite homogeneous and yield very weak luminescence, whereas for old or improperly preserved samples, the surface luminescence overwhelms the Raman signal. We employed true backscattering geometry at room temperature in air for all measurements shown here. Additional low-temperature

measurements used a pseudo backscattering geometry in a flowing helium cryostat. The raw data were corrected for the spectral response of the equipment using a standard lamp and are plotted in units proportional to a photon cross section. All data were normalized to the same flux of incident laser photons, corresponding to a power density of approximately 4 MW/m^2.

Figure 1 shows Raman spectra for Gd_2CuO_4 in various true backscattering configurations, where the z axis was along the crystal c axis, the unprimed x and y were along the in-plane Cu-O bonds, and the primed x' and y' axes were rotated 45° with respect to them. A well-defined Raman peak at around 1.5 eV, with half-width about 0.2 eV, was observed for the first time. This feature appears only for crossed polarizations, $\mathbf{e}_L \times \mathbf{e}_S$, indicating that this excitation has the symmetry of a pseudovector, A_{2g}. Confirmation of this unusual symmetry is provided by measurements with circularly polarized light. In addition, two weaker features are also resolved in A_{1g} and B_{1g} symmetries. The A_{1g} feature appears at a slightly lower energy than that of the A_{2g} peak, while the B_{1g} feature appears at about 1.7 eV, coinciding with the position of the strong optical absorption peak. Low temperature measurements (not shown here) indicated that the A_{2g} peak narrows significantly with decreasing temperature, but does not shift in position.

In order to see whether these excitations are universal for insulating cuprates, we studied other T'-phase samples with R=Eu, Sm, Nd, as well as $YBa_2Cu_3O_{6.1}$ and $PrBa_2Cu_3O_{6.1}$. The systematic study of the T' samples will be published elsewhere [14]. In Fig. 2, we plot the A_{2g} spectra for Gd_2CuO_4, Nd_2CuO_4, $YBa_2Cu_3O_{6.1}$, and $PrBa_2Cu_3O_{6.1}$ along with their corresponding optical absorption spectra. In all cases, the A_{2g} peak position occurs on the structureless absorption edge below the strong peak in ε_2. The B_{1g} Raman feature, as shown in Fig. 1 for Gd_2CuO_4, is also observed to occur at the same energy as that of the ε_2 peak in all of our other samples (not shown here). However, the A_{1g} feature observed in Gd_2CuO_4 is not as universal; its intensity changes among the T' samples, and it can hardly be resolved in $YBa_2Cu_3O_{6.1}$.

Figure 2 shows two very interesting trends. First, the overall positions of the A_{2g} peak and the ε_2 peak shift together with changes in the Cu-O bond length. In Fig. 2, they are quite similar for the pairs Gd_2CuO_4 (1.948 Å) and $YBa_2Cu_3O_{6.1}$ (1.941 Å [15]), and Nd_2CuO_4 (1.973 Å) and $PrBa_2Cu_3O_{6.1}$ (1.962 Å [16]). Second, the separation of the A_{2g} Raman peak from the ε_2 peak is similar for materials with the same Cu coordination number. The A_{2g} Raman peak appears roughly 0.2 eV below the ε_2 peak for the T' samples with square-planar coordinated Cu sites, while it is 0.15 eV below for the "123" cuprates with pyramidally coordinated Cu sites. Measurements on La_2CuO_4, which has octahedrally coordinated Cu sites, are planned to check whether the Cu coordination number trend continues.

Our measurements with different laser lines not only

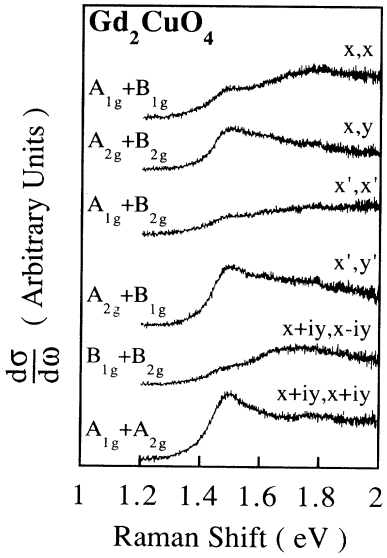

FIG. 1. Raman spectra of Gd_2CuO_4, excited at 3.81 eV, in six different scattering configurations $z(\mathbf{e}_L,\mathbf{e}_S)\bar{z}$.

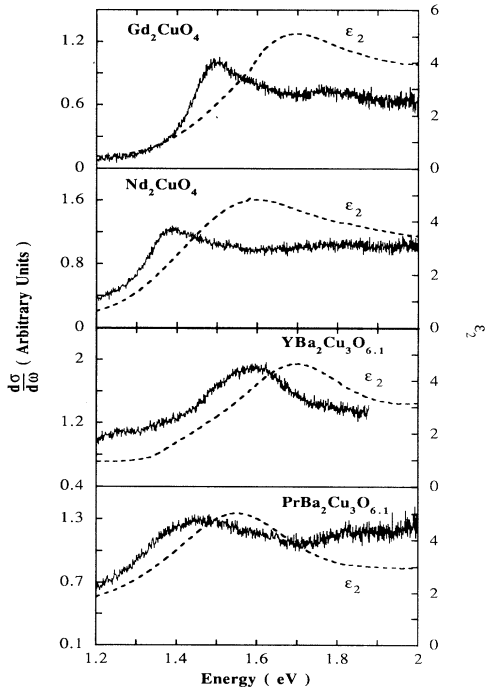

FIG. 2. Raman spectra (in Raman shift) and ε_2 (in photon energy) for four different insulating cuprates. The Raman spectra were taken in the $z(x+iy,x+iy)\bar{z}$ geometry (probing A_{2g} plus weak A_{1g} components) with 3.81 eV excitation. The spectra show varying amounts of luminescence and stray light in the background, but peak positions are not affected.

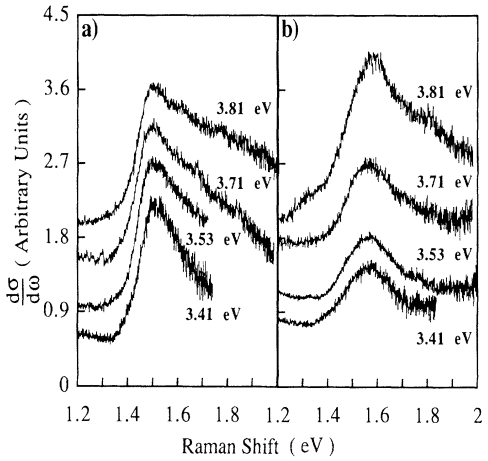

FIG. 3. The $z(x,y)\bar{z}$ Raman spectra of (a) Gd_2CuO_4 and (b) $YBa_2Cu_3O_{6.1}$ excited at four different laser energies. Since the B_{2g} signal is negligible, the Raman mode is of almost pure A_{2g} symmetry. The upper three curves in (a) have been raised by 0.3 (3.53 eV), 0.8 (3.71 eV), and 1.6 (3.81 eV) units for clarity. In (b), the curves have not been offset; the varying background levels are due to the presence of intrinsic luminescence. The spectra have been normalized to the same number of incident laser photons.

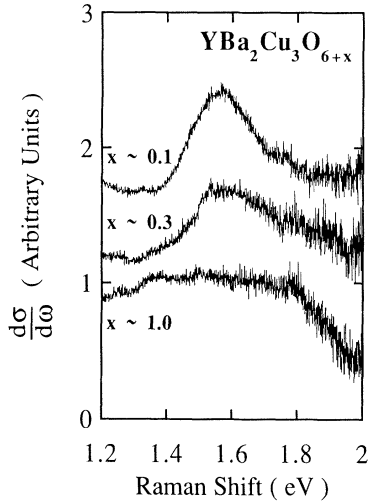

FIG. 4. The $z(x,y)\bar{z}$ Raman spectra of $YBa_2Cu_3O_{6+x}$ at three different doping levels. The upper two curves are raised by 0.5 ($x\sim0.3$) and 0.6 ($x\sim0.1$) intensity units for clarity.

confirmed the Raman nature of these spectral features, but also revealed their resonance behavior. Figure 3 shows that the A_{2g} features for Gd_2CuO_4 and $YBa_2Cu_3O_{6.1}$ seem to resonate weakly in intensity towards higher photon energy, while their positions remain almost constant for incident photons in the range of 3.41 to 3.81 eV. Recently Wake [17] has also performed a resonance experiment on $YBa_2Cu_3O_{6.1}$, observing a peak similar in energy to our A_{2g} peak. However, this feature does not have a clear polarization dependence, and it shifts more than 800 cm^{-1} in position for laser energies varying from 3.4 to 3.6 eV. Despite much effort, we have been unable to reproduce these results.

Figure 4 shows the doping dependence of the A_{2g} peak for $YBa_2Cu_3O_{6+x}$. The feature is distinct and remains unchanged in position for $x\sim0.1$ and $x\sim0.3$ samples, disappearing in metallic $x\sim0.6$ (not shown) and $x\sim1.0$ samples.

The microscopic origin of the A_{2g} excitation is unclear. Its special symmetry, transforming as $xy-yx$, $xy(x^2-y^2)$, or a pseudovector L_z, and its energy suggest two likely scenarios: (1) an intra-atomic $d_{x^2-y^2}\rightarrow d_{xy}$ hole transition, or (2) an interatomic transition, e.g., from a hole in a d orbital (or a linear combination of d orbitals on different sites) having symmetry (x^2-y^2) to a linear combination of $O(p)$ orbitals having symmetry (xy). A less conventional model might posit an excitation from a state where the Néel symmetry is locally broken due to quantum fluctuations, e.g., of a chiral nature [6,18]. Detailed theoretical studies of these (and maybe other) possibilities may be necessary to determine the correct explanation.

The first scenario involves valence-conserving d-d transitions, which are parity forbidden for an electric dipole transition but parity allowed for Raman scattering. Electronic Raman scattering has successfully probed crystal-field splitting of d^6 (Fe^{2+}) [19], d^7 (Co^{2+}), and d^8 (Ni^{2+}) [20]. However, to our knowledge, crystal field transitions have not been observed by Raman scattering on a d^9 (Cu^{2+}) configuration. It is well known that a D_{4h} tetragonal crystal field will split the d^9 (Cu^{2+}) orbitals into states with representations b_{1g} (x^2-y^2), $a_{1g}(3z^2-r^2)$, $b_{2g}(xy)$, and $e_g(xz,yz)$. The three d^9-d^9 excitations, $d_{x^2-y^2}\rightarrow d_{xy}$, $d_{x^2-y^2}\rightarrow d_{3z^2-r^2}$, and $d_{x^2-y^2}\rightarrow d_{xz}(d_{yz})$, have A_{2g} $(b_{1g}\times b_{2g}=a_{2g})$, B_{1g} $(b_{1g}\times a_{1g}=b_{1g})$, and E_g $(b_{1g}\times e_g=e_g)$ symmetries, respectively. Our A_{2g} Raman feature corresponds well to the $d_{x^2-y^2}\rightarrow d_{xy}$ transition, having both the correct symmetry and an energy comparable to that yielded by cluster calculations (~1.7 eV) [21]. The intermediate hole states participating in this Raman process could be an admixture of O p_σ and p_π orbitals hybridizing with different crystal-field-split d^9 wave functions.

The B_{1g} Raman feature might also correspond to a d-d transition. This would amount to a variation on a suggestion by Perkins *et al.* [22]. Our weak B_{1g} Raman feature coinciding with the absorption peak near 2 eV could be assigned to the $d_{x^2-y^2}\rightarrow d_{3z^2-r^2}$ transition. In this interpretation, it is unclear why our B_{1g} feature would be so weak compared with the A_{2g} peak, and why the B_{1g} feature should follow the E_u absorption peak so closely.

The second scenario involves models for CT excitons with A_{2g}, B_{1g}, and E_u symmetries. One model A_{2g} exciton is formed out of the Néel state due to the effects of a photon-assisted $d\rightarrow p_\sigma$ transition followed by photon-

assisted $p_\sigma \rightarrow p_\pi$ hole hopping. In this way, one can obtain a vacant $d_{x^2-y^2}$ hole at site (0,0) and a linear combination of $p_\pi(\mathbf{r})$ holes at nearest-neighbor sites $\mathbf{r}$ having b_{2g} symmetry:

$$P(b_{2g}) \equiv \tfrac{1}{2}[p_{\pi x}(0,1) - p_{\pi x}(0,-1) + p_{\pi y}(1,0) - p_{\pi y}(-1,0)], \quad (1)$$

where the components of $\mathbf{r}$ are given in units of the Cu-O bond length. This O-hole orbital will couple by $p_\pi \leftrightarrow d_{xy}$ hopping to the d_{xy} orbital at (0,0). It will also couple to a hole state of b_{2g} symmetry composed of a linear combination of the eight second-neighbor p_σ orbitals at $\mathbf{r} = (\pm 1, \pm 2), (\pm 2, \pm 1)$. Some computational work is necessary to estimate the energy and wave function of the lowest resulting b_{2g} state.

A CT exciton of B_{1g} symmetry can be formed out of the Néel state due to the effects of a photon-assisted $d \rightarrow p_\sigma$ transition followed by photon-assisted $p_\sigma \rightarrow p_\sigma$ hole hopping. One obtains a vacant $d_{x^2-y^2}$ hole at site (0,0) and a linear combination of $p_\sigma(\mathbf{r})$ holes at nearest neighbor sites $\mathbf{r}$ having a_{1g} symmetry:

$$P_\sigma(a_{1g}) \equiv \tfrac{1}{2}[p_{\sigma x}(1,0) - p_{\sigma x}(-1,0) + p_{\sigma y}(0,1) - p_{\sigma y}(0,-1)]. \quad (2)$$

Optical absorption can occur through charge transfer excitations of $E_u(x)$ symmetry from the $d_{x^2-y^2}$ hole at site (0,0) to p_σ states or p_π states, respectively:

$$P_{\sigma x} \equiv (1/\sqrt{2})[p_{\sigma x}(1,0) + p_{\sigma x}(-1,0)], \quad (3)$$

$$P_{\pi x} \equiv (1/\sqrt{2})[p_{\pi x}(0,1) + p_{\pi x}(0,-1)]. \quad (4)$$

We expect (3) and (4) to be coupled due to $p_\pi \leftrightarrow p_\sigma$ hole hopping.

The existence of an exciton of A_{1g} symmetry has not been as firmly established in the present work as those of A_{2g} and B_{1g} symmetries. It could result from transfer of $d_{x^2-y^2}$ hole at site (0,0) to p_σ states at a linear combination of $p_\sigma(\mathbf{r})$ holes at nearest-neighbor sites $\mathbf{r}$ having b_{1g} symmetry:

$$P_\sigma(b_{1g}) \equiv \tfrac{1}{2}[p_{\sigma x}(1,0) - p_{\sigma x}(-1,0) - p_{\sigma y}(0,1) + p_{\sigma y}(0,-1)]. \quad (5)$$

The d-p charge transfer picture has the advantage of being able to produce excitations of A_{2g}, B_{1g}, E_u, and A_{1g} symmetry by the simple act of hole transfer to nearest-neighbor sites, as described by Eqs. (1)–(5), but d-d transitions may play primary or secondary roles in some of these excitations.

In summary, we have discovered several Raman-active electronic transitions near the CT gap in the insulating cuprates. They are suppressed by doping the CuO_2 plane, and vanish in the metallic phase. We believe that the A_{2g} Raman feature corresponds well to the spin-allowed and valence-conserving $d_{x^2-y^2} \rightarrow d_{xy}$ excitation, or alternatively, the peak might represent a CT exciton with compatible symmetry and energy. Clearly, these new Raman modes together with recent RRS results [11] show that the CuO_2 planes of the insulating cuprates have exciton-like excitations of considerable complexity.

We thank the NSF for support under DMR 90-17156 (R.L., D.S., M.V.K.) and under DMR 91-2000 (R.L., S.L.C., M.V.K., W.C.L., D.M.G.).

*Present address: Department of Physics, University of Maryland, College Park, MD 20742.

[1] P. W. Anderson, Science **235**, 1196 (1987).
[2] F. C. Zhang and T. M. Rice, Phys. Rev. B **37**, 3759 (1988); C. M. Varma, S. Schmitt-Rink, and E. Abrahams, Solid State Commun. **621**, 681 (1987); V. J. Emery, Phys. Rev. Lett. **58**, 2794 (1987).
[3] W. Weber, Z. Phys. B **70**, 323 (1988).
[4] See, for example, D. Vaknin *et al.*, Phys. Rev. Lett. **58**, 2802 (1987); J. M. Tranquada *et al.*, Phys. Rev. Lett. **60**, 156 (1988); B. Keimer *et al.*, Phys. Rev. B **46**, 14034 (1992).
[5] P. W. Anderson, G. Baskaran, Z. Zhou, and T. Hsu, Phys. Rev. Lett. **58**, 2790 (1987).
[6] I. Affleck and J. M. Marston, Phys. Rev. B **37**, 3774 (1988); R. B. Laughlin, Science **242**, 525 (1988).
[7] N. Nüker *et al.*, Phys. Rev. B **39**, 6619 (1989); M. Alexander *et al.*, Phys. Rev. B **43**, 333 (1991).
[8] For a review, see D. B. Tanner and T. Timusk, in *Physical Properties of High Temperature Superconductors III*, edited by D. M. Ginsberg (World Scientific, Singapore, 1992).
[9] E. T. Heyen, J. Kircher, and M. Cardona, Phys. Rev. B **45**, 3037 (1992).
[10] M. Yoshida *et al.*, Phys. Rev. B **46**, 6505 (1992).
[11] Ran Liu *et al.*, in Proceedings of the Conference on Spectroscopies in Novel Superconductors, Santa Fe, New Mexico [J. Phys. Chem. Solids (to be published)].
[12] D. Salamon *et al.*, Poster M99, contribution to the American Physical Society March Meeting, Seattle, Washington, 1993 (unpublished).
[13] J. P. Rice and D. M. Ginsberg, J. Cryst. Growth **109**, 432 (1991); W. C. Lee and D. M. Ginsberg, Phys. Rev. B **44**, 2815 (1991); S.-W. Cheong, J. D. Thompson, and Z. Fisk, Physica (Amsterdam) **158C**, 109 (1989).
[14] D. Salamon *et al.* (to be published).
[15] R. M. Hazen, in *Physical Properties of High Temperature Superconductors II*, edited by D. M. Ginsberg (World Scientific, Singapore, 1990), p. 121.
[16] A. K. Ganguli *et al.*, Z. Phys. B **74**, 215 (1989).
[17] D. R. Wake (unpublished).
[18] X. G. Wen, F. Wilczek, and A. Zee, Phys. Rev. B **39**, 11413 (1989).
[19] R. M. Macfarlane, Solid State Commun. **15**, 535 (1974).
[20] A. T. Abdalian and P. Moch, J. Phys. C **19**, 7307 (1986); **21**, 767 (1988).
[21] A. K. McMahan, R. M. Martin, and S. Satpathy, Phys. Rev. B **38**, 6650 (1988); R. L. Martin, in *Cluster Models for Surface and Bulk Phenomena*, edited by G. Pacchioni *et al.* (Plenum, New York, 1992), p. 485.
[22] J. D. Perkins *et al.*, Phys. Rev. Lett. **71**, 1621 (1993).